Causal Relationship between the Loss of *RUNX3* Expression and Gastric Cancer

Qing-Lin Li,[1,12] Kosei Ito,[2,12] Chohei Sakakura,[3,12]
Hiroshi Fukamachi,[4,12] Ken-ichi Inoue,[2] Xin-Zi Chi,[1]
Kwang-Youl Lee,[1] Shintaro Nomura,[5]
Chang-Woo Lee,[6] Sang-Bae Han,[6]
Hwan-Mook Kim,[6] Wun-Jae Kim,[7]
Hiromitsu Yamamoto,[2] Namiko Yamashita,[2]
Takashi Yano,[2] Toshio Ikeda,[8,13] Shigeyoshi Itohara,[8,13]
Johji Inazawa,[9] Tatsuo Abe,[3] Akeo Hagiwara,[3]
Hisakazu Yamagishi,[3] Asako Ooe,[2]
Atsushi Kaneda,[10] Takashi Sugimura,[10]
Toshikazu Ushijima,[10] Suk-Chul Bae,[1,11]
and Yoshiaki Ito[2,11]
[1] Department of Biochemistry
College of Medicine
Institute of Medical Research
Chungbuk National University
Cheongju 361-763, South Korea
[2] Department of Viral Oncology
Institute for Virus Research
Kyoto University
Sakyo-ku, Kyoto 606-8507, Japan
[3] Department of Digestive Surgery
Kyoto Prefectural University of Medicine
Kamigyo-ku, Kyoto 602-0841, Japan
[4] Department of Biological Sciences
Graduate School of Science
University of Tokyo
Hongo
Bunkyo-ku, Tokyo 113-0033, Japan
[5] Department of Pathology
Graduate School of Medicine
Osaka University
Suita, Osaka 565-0871, Japan
[6] Korea Research Institute of Bioscience
   and Biotechnology
Yusung, Taejon 305-600, South Korea
[7] Department of Urology
College of Medicine
Chungbuk National University
Cheongju 361-763, South Korea
[8] Laboratory of Advanced Biological Information
Institute for Virus Research
Kyoto University
Sakyo-ku, Kyoto 606-8507, Japan
[9] Medical Research Institute
Tokyo Medical and Dental University
Yushima
Bunkyo-ku, Tokyo 113-8510, Japan
[10] National Cancer Center Research Institute
Tsukiji
Chuo-ku, Tokyo 104-0045, Japan

[11] Correspondence: scbae@med.chungbuk.ac.kr (S.C.B.), yito@virus.
kyoto-u.ac.jp (Y.I.)
[12] These four authors contributed equally to this work.
[13] Present address: Laboratory for Behavioral Genetics, Brain Science Institute, RIKEN, 2-1 Hirosawa, Wako, Saitama 351-0198, Japan.

Summary

Runx3/Pebp2αC null mouse gastric mucosa exhibits hyperplasias due to stimulated proliferation and suppressed apoptosis in epithelial cells, and the cells are resistant to growth-inhibitory and apoptosis-inducing action of TGF-β, indicating that *Runx3* is a major growth regulator of gastric epithelial cells. Between 45% and 60% of human gastric cancer cells do not significantly express *RUNX3* due to hemizygous deletion and hypermethylation of the *RUNX3* promoter region. Tumorigenicity of human gastric cancer cell lines in nude mice was inversely related to their level of *RUNX3* expression, and a mutation (R122C) occurring within the conserved Runt domain abolished the tumor-suppressive effect of *RUNX3*, suggesting that a lack of *RUNX3* function is causally related to the genesis and progression of human gastric cancer.

Introduction

Gastric cancer is the most frequent malignancy of the gastrointestinal tract in Japanese and certain Southeast Asian populations and the second most common cause of cancer-related death in the world (Parkin et al., 1997, 1999).

Genetic alterations associated with gastric cancer have been described, such as a loss of the genes encoding E cadherin (Guilford et al., 1998), p53 (Kim et al., 1991; Tamura et al., 1991), or the transforming growth factor-β (TGF-β) receptor (Park et al., 1994) or overexpression of *erbB-2* (Fukushige et al., 1986) or *c-met* (Rege-Cambrin et al., 1992), but they have only been found to be associated with a limited number of cases. Chromosomal aberrations in gastric cancer have been extensively studied, and the loss of many chromosomal loci has been discovered, including the loss of 1p, 5q, 7q, 12q, 17p, and 18q (Sano et al., 1991; Uchino et al., 1992; Kuniyasu et al., 1994); however, the significance of each of these changes, let alone the identity of the specific genes involved, is unclear. Therefore, the underlying mechanism of gastric carcinogenesis is still poorly understood.

TGF-β is a multifunctional growth factor that has profound regulatory effects on many developmental and physiological processes. It is interesting to note that, in the *TGF-β1* null animals, gastric epithelial proliferation is stimulated and epithelial hyperplasia is found, together with numerous anomalies reflecting its multifunctional properties (Crawford et al., 1998). Thus, TGF-β may be a factor that regulates the gut development.

Runt domain transcription factors, also called the polyomavirus enhancer binding protein 2/core binding factors (PEBP2/CBF), are important targets of TGF-β superfamily signaling and play crucial roles in mammalian development. PEBP2 is a heterodimeric complex composed of α and β subunits (Ito, 1999). The α subunit is homologous to the product of the *Drosophila* segmentation genes *runt* and *lozenge* and contains a conserved

region termed the Runt domain, which is required for dimerization with the β subunit and for recognition of the cognate DNA binding sequence. There are three mammalian *runt*-related genes, *RUNX1/AML1*, *RUNX2/CBFA1*, and *RUNX3/PEBP2αC/AML2*. RUNX proteins form complexes with Smad2 and Smad3 that transmit TGF-β/activin signals (Hanai et al., 1999). *RUNX1* is required for definitive hematopoiesis (Okuda et al., 1996). It is the most frequent target of chromosome translocation in leukemia and is responsible for about 30% of human acute leukemia cases (Look, 1997). *RUNX2* is essential for osteogenesis. Its haploinsufficiency causes the human bone disease cleidocranial dysplasia (Lee et al., 1997; Mundlos et al., 1997).

In this communication, we show that the *Runx3$^{-/-}$* mouse gastric mucosa exhibits hyperplasias due to the stimulated proliferation and suppressed apoptosis in the cells. This line of evidence suggests that *RUNX3* is an attractive candidate as a tumor suppressor of gastric cancer and prompted us to investigate this possibility. Indeed, we found that *RUNX3* possesses a potent anti-oncogenic activity and is frequently inactivated in gastric cancers by hemizygous deletion and hypermethylation of its promoter region.

Results

Targeted Disruption of the *Runx3* Locus in Mice

The strategy used to inactivate *Runx3* in the mouse germline is described in Figure 1A. In order to follow the expression of *Runx3*, the *lacZ* reporter sequence was inserted in frame into the *Runx3* gene. The presence of the null *Runx3* alleles in the newborn mice was confirmed by genomic Southern blot analysis (Figure 1B).

Runx3 Is Expressed in Gastrointestinal Epithelial Cells

In the *Runx3$^{+/-}$* mouse fetus, which developed normally without apparent defects, β-galactosidase (β-gal) activity could be detected histochemically. At 12.5 days post coitus (dpc), β-gal activity in the *Runx3$^{+/-}$* mouse was found in the cartilage in limbs and the nasal cavity, in trigeminal (Figure 1C) and dorsal root ganglia (Figure 1D). Strong β-gal activity was found in gastrointestinal organs, including the stomach and the small and large intestines, from 14.5 dpc (Figure 1E) through to adulthood. In this study, we will focus our analysis on the stomach, where *Runx3* is strongly expressed.

In situ hybridization on the newborn stomach showed that there was strong expression in epithelial cells of the glandular stomach but only very weakly in the forestomach epithelia (Figure 1F). In the adult stomach, expression was greater in chief and surface mucous cells than in the parietal cells (Figures 1H and 1I). Only weak signals could be found in the stem cell zone where proliferating cells could be labeled with 5-bromo-2'-deoxyuridine (BrdU) (Figures 1I and 1K).

Hyperplasia and Increased Epithelial Proliferation in *Runx3$^{-/-}$* Gastric Mucosa

When *Runx3$^{+/-}$* mice were mated, about 20%–25% of newborn mice were *Runx3$^{-/-}$*. Newborn mice had no genotype-dependent differences in body weight, size, or response to the mother. However, *Runx3$^{-/-}$* mice died soon after birth. In the first day after birth, 75% of *Runx3$^{-/-}$* mice died, and none survived beyond 10 days. Blood sugar levels in *Runx3$^{-/-}$* mice were very low and therefore, knockout mice may have died by starvation. We noted that the stomach wall of *Runx3$^{-/-}$* mice was thicker than that of wild-type (wt) animals. We thus compared the gastric tissue structures by fixing the stomachs just after parturition before suckling commenced.

In the fundic area near the forestomach, the gland was more elongated in the knockout mice than wt animals. Thus, the stomach mucosa of *Runx3$^{-/-}$* mice is about twice as thick as that of wt mice (Figures 2A and 2B), suggesting that disruption of *Runx3* results in hyperplasia of the gastric mucosa. Immunohistochemical analysis of gastric epithelial proliferation by labeling 18.5 dpc cells with BrdU showed that replicating cells were localized at the gland base in both *Runx3$^{-/-}$* and wt mice (Figures 2C and 2D) and that the labeling index was significantly greater in the *Runx3$^{-/-}$* mouse than in wt mice in both the fundic and pyloric areas ($p < 0.05$; Figure 2E). This indicates that gastric epithelial proliferation was stimulated by the disruption of *Runx3*.

Runx3$^{-/-}$ Gastric Epithelial Cells Are Less Sensitive to the Growth-Inhibitory Effect of TGF-β

The observations that disruption of *Runx3* resulted in increased proliferation and hyperplasia of gastric epithelial cells, albeit not as severely as in *TGF-β1* null mice, suggest a link between TGF-β and *Runx3*. To examine whether hyperplasia and increased epithelial proliferation in *Runx3$^{-/-}$* gastric mucosa were due to impaired TGF-β signaling pathway in the epithelial cells in a cell-autonomous fashion rather than the influence from surrounding mesenchyme, the response of 18.5 dpc gastric epithelial cells to TGF-β was examined in primary culture.

The high purity of the gastric epithelial cell populations without mesenchymal contamination was confirmed (Figure 2F). The epithelial cells from both wt and *Runx3$^{-/-}$* mice proliferated rapidly in culture, and wt epithelial cell growth was significantly inhibited by TGF-β1 (Figure 2G). In contrast, *Runx3$^{-/-}$* epithelial cell growth was less severely inhibited (Figure 2H), and the difference between wt and *Runx3$^{-/-}$* cells was significant ($p < 0.05$).

Gastric Epithelial Apoptosis Is Suppressed in *Runx3$^{-/-}$* Mice

That *Runx3$^{-/-}$* gastric epithelial cells are less sensitive to TGF-β than wt cells suggests that gastric epithelial apoptosis may also be altered in *Runx3$^{-/-}$* mice. We thus examined epithelial apoptosis in the developing gastrointestinal organs by the TdT-mediated dUTP-biotin nick-end labeling (TUNEL) method.

In the newborn wt mouse, apoptotic cells were observed in esophageal epithelial cells lining the luminal surface (Figure 3A) and in gastric epithelial cells on the surface of glandular structures (Figures 3C and 3E). In the newborn *Runx3$^{-/-}$* mouse, apoptosis was found in esophageal epithelial cells facing the lumen (Figure 3B), but no apoptotic cells were found in *Runx3$^{-/-}$* gastric epithelium (Figures 3D and 3F). Consistent with this,
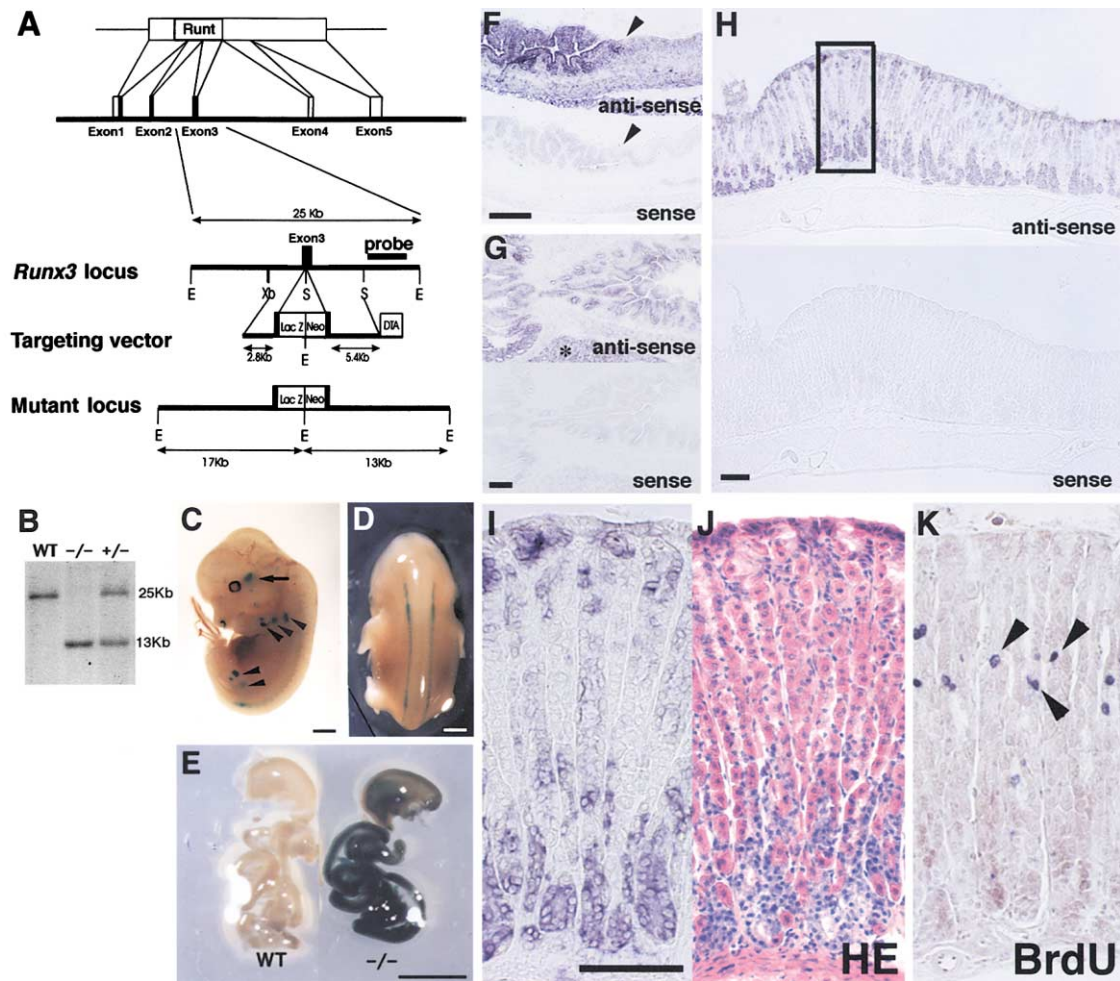
Figure 1. Targeted Disruption of *Runx3* and Expression of *Runx3*

(A) Genomic structure of *Runx3*, the structure of the targeting vector for homologous recombination, and the gene structure of the targeted locus. Exons are indicated by boxes. A probe (shown on *Runx3* locus) is used in genomic Southern blot analysis. Abbreviations: Runt, the Runt domain; E, *Eco*R1; Xb, *Xba*I; S, *Sma*I; Neo, neo-resistant gene.

(B) Southern blot analysis of genomic DNAs of wt, *Runx3*$^{-/-}$ ($-/-$), and *Runx3*$^{+/-}$ ($+/-$) mice, detected by the probe shown in (A).

(C and D) Whole-mount β-gal staining of a 12.5 dpc *Runx3*$^{+/-}$ fetal mouse. In (C), positive reaction is depicted by an arrow, and arrowheads indicate the trigeminal ganglion and the cartilage in the limb buds. In (D), a positive reaction in the bilateral dorsal root ganglia is shown. Scale bars are equal to 1 mm.

(E) Whole-mount β-gal staining of resected gastrointestinal tracts from 14.5 dpc fetal mice. Note that whole *Runx3*$^{-/-}$ tissues apart from the forestomach were positively stained. Scale bar is equal to 1 mm.
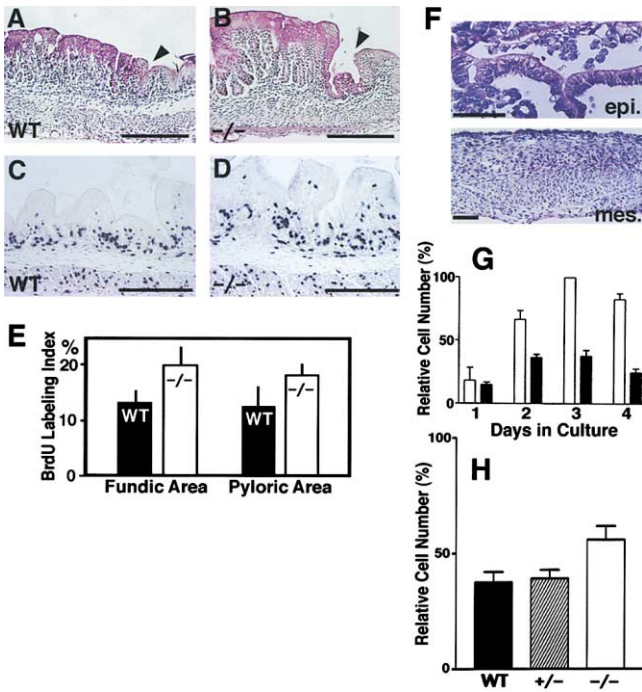
(F–I) Detection of *Runx3* mRNA by in situ hybridization in the stomach (F) and the junction between the stomach and intestine (G) of a newborn mouse and in the glandular stomach (H) of a 10-week-old mouse. In (F), the border between the glandular stomach (left) and forestomach (right) is shown by arrowheads. In (G), the pylorus (right) and duodenum (left) can be distinguished, and the liver is indicated by an asterisk. A rectangle in (H) is enlarged and shown in (I). Scale bars are equal to 100 μm.

(J and K) Hematoxylin and eosin (HE) staining (J) and immunohistochemical detection of replicating cells (K) in sections similar to the region shown in (I). Arrowheads in (K) indicate BrdU-incorporated nuclei.

caspase 3 was not activated in *Runx3*$^{-/-}$ mouse gastric tissues (Figures 3G and 3H). These observations suggest that *Runx3* is essential in inducing apoptosis in gastric epithelial cells and that the epithelial hyperplasia in the *Runx3*$^{-/-}$ glandular stomach results, at least in part, from reduced apoptosis of the epithelial cells.

We then investigated the effect of TGF-β on gastric epithelial apoptosis in primary cell culture. In this experiment, TGF-β1 was added to the culture medium on day 4 when spontaneous apoptosis could be observed. Since apoptotic cells became round in shape and easily

detached from the substratum to float in the culture media, it was rare to find TUNEL-positive substratum-attaching cells in control cultures (Figure 3J). When wt cells were treated with TGF-β1, however, many substratum-attaching cells were found to be TUNEL positive (Figure 3N). In cultures of *Runx3*$^{-/-}$ gastric epithelial cells, in contrast, TUNEL-positive cells could not be observed even if they were treated with TGF-β (Figures 3L and 3P). We thus concluded that TGF-β1 induces apoptosis in gastric epithelial cells in primary culture and that *Runx3*$^{-/-}$ gastric epithelial cells are resistant

Figure 2. The Growth Regulation of Gastric Epithelial Cells by *Runx3* and TGF-β

(A and B) Light micrographs of the fundic area in the stomach from mice fixed just after birth before suckling, stained with periodic-acid Schiff (PAS) reaction and hematoxylin. The border of the glandular stomach (left) and the forestomach (right) is indicated by arrowheads. Scale bars are equal to 100 μm.

(C and D) Immunohistochemical detection of replicating cells in the stomach from 18.5 dpc fetal mice. Scale bars are equal to 100 μm.

(E) Quantitative analysis of gastric epithelial proliferation. The labeling index was calculated as a percentage of BrdU-labeled cells in the total epithelial cell populations from 18.5 dpc fetal gastric tissues. Mean ± SD of five fetuses.

(F) Light micrographs of epithelial (epi) and mesenchymal (mes) components from 18.5 dpc glandular stomach tissues fixed just after separation by EDTA treatment and stained with PAS and hematoxylin. Scale bars are equal to 50 μm.

(G) Growth of glandular stomach epithelial cells in TGF-β1 (3 ng/ml)-supplemented (black bars) or in control (open bars) medium during primary culture. The number of cells in control medium on day 3 was regarded as 100%.

Mean ± SD of 4–6 determinations.

(H) Relative number of gastric epithelial cells on day 3 of culture in TGF-β1-supplemented media. The cell number in the control medium is regarded as 100%.

to this apoptosis-inducing action of TGF-β. These observations prompted us to examine whether *RUNX3* is involved in human gastric cancer.

Hemizygous Deletion of *RUNX3*
First, we examined the integrity of the *RUNX3* gene in 15 gastric cancer cell lines by fluorescent in situ hybrid-

ization (FISH). Most cell lines exhibited aneuploidy, having two, three, or more copies of chromosome 1 as revealed by a centromere-specific probe (green spots in Figure 4A). The numbers of copies of chromosome 1 and *RUNX3* were counted, and *RUNX3*/centromere spot ratio was determined. The ratio was always 1 (2/2) in normal peripheral lymphocytes, but was less than 1 in
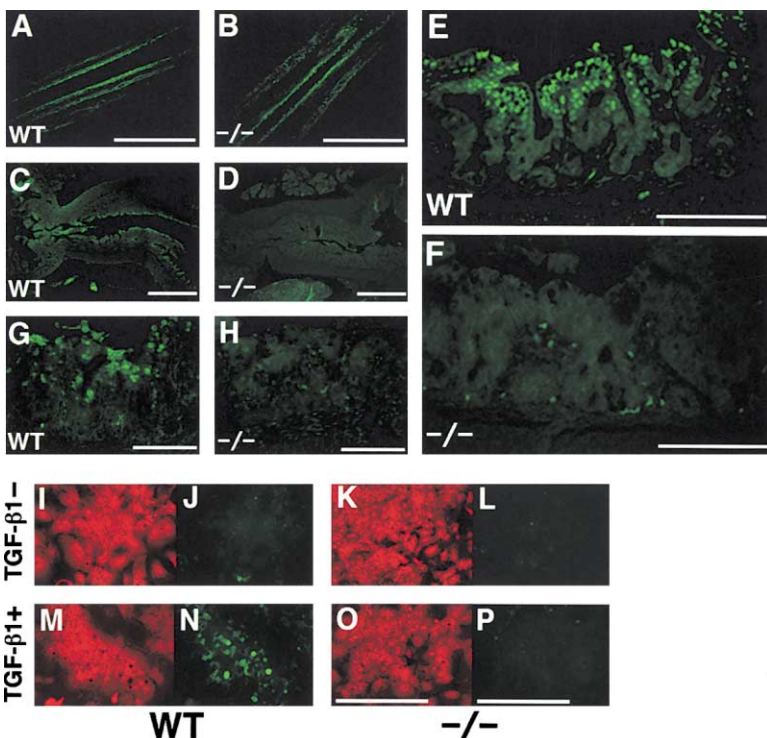

Figure 3. Detection of Apoptotic Cells by TUNEL

(A–H) Fluorescent micrographs of esophageal (A and B) and pyloric (C–H) tissues from newborn mice. (E) and (F) are higher magnifications of sections in (C) and (D), respectively. TUNEL-positive nuclei (A–F) are stained in green. Immunohistochemical detection of active-caspase 3 (G and H). Scale bars in (A)–(D) are equal to 500 μm and in (E)–(H) are equal to 100 μm.

(I–P) Gastric epithelial cells from wt (I, J, M, and N) and *Runx3*⁻/⁻ (K, L, O, and P) fetal mice in primary culture, treated with TGF-β1 (M–P) or vehicle (I–L) and double-stained with TUNEL and with propidium iodide. The same area is shown in two accompanying figures to show the location of TUNEL-positive nuclei (J, L, N, and P) among all the nuclei (I, K, M, and O). Scale bars are equal to 100 μm.

A

control   SNU1

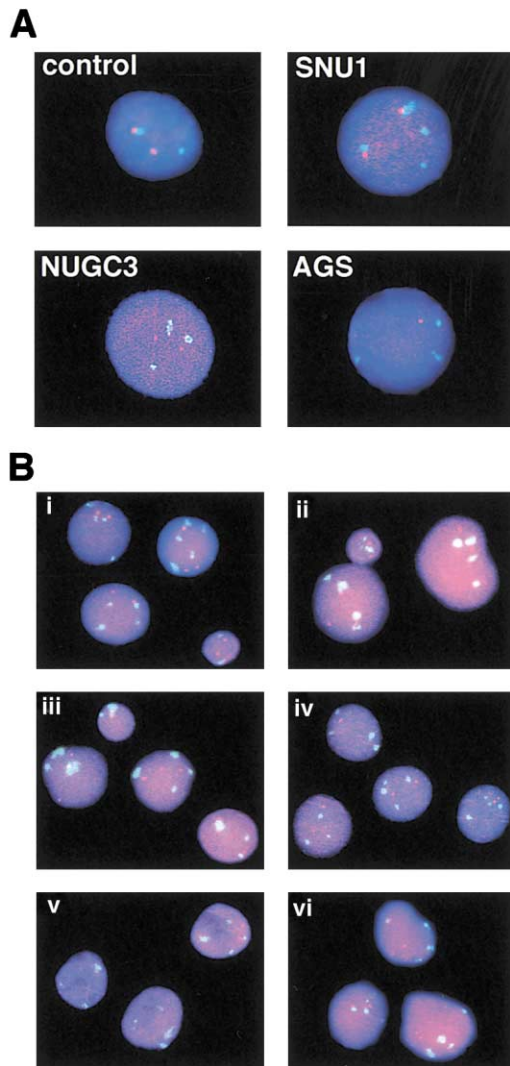NUGC3   AGS

B

i   ii

iii   iv

v   vi

Figure 4. Hemizygous Deletions of *RUNX3* in Gastric Cancer Cells

(A) Bicolor FISH analysis of *RUNX3* in gastric cancer cell lines using a centromere-specific probe (green) and a *RUNX3*-specific probe (red). Peripheral blood lymphocytes were used as a normal cell control.

(B) Bicolor FISH analysis of *RUNX3* from surgically resected primary gastric cancer cells obtained from five tumors (i, ii, iii, iv, and vi) and one liver metastasis (v).

some cell lines. In SNU1 and NUGC3 cells, the ratio was 2/4 in most cells (71% and 73% of total cell populations, respectively), while it was 2/3 in 48% and 1/3 in 42% of the AGS cell population (Figure 4A). Out of the 15 cell lines tested, these three cell lines were considered to have hemizygous deletions of *RUNX3*.

Next, we looked for hemizygous deletions of *RUNX3* by FISH in 46 surgically resected primary cancer specimens. Six representative FISH analyses are shown in Figure 4B. Tumor cells from these primary cancers also displayed aneuploidy, and the *RUNX3*/centromere ratio was less than 1 in all cases (Figure 4B). A biallelic deletion of *RUNX3* was observed in some of the metastatic tumor cells (Figure 4B, v). Progression of gastric cancer has been classified into four stages, from I through IV, depending on the depth of tumor invasion, metastasis

into the lymph node or liver, and peritoneal dissemination according to the UICC classification (Sobin and Wittekind, 1997). Of the 46 specimens examined, 14 cases (30%) showed a hemizygous deletion of *RUNX3*, including 3 out of 22 stage I (14%), none out of 2 stage II, 3 out of 14 stage III, and 8 out of 8 stage IV cases (100%). The proportion of hemizygous deletions significantly increased as the cancer progressed to more advanced stages ($p < 0.01$ examined by Mann-Whitney U test).

Frequent Loss of *RUNX3* Expression
We then examined the expression of *RUNX3* in gastric cancer cell lines by the reverse transcriptase-polymerase chain reaction (RT-PCR) and found that expression of *RUNX3* was undetectable in six cell lines (SNU1, NUGC3, MKN28, MKN74, AGS, and KATOIII), including those with hemizygous deletions of *RUNX3* (Figure 5A). The expression level was very low in MKN7 cells (Figure 5A). Southern blot analysis of the amplified DNA using the *RUNX3* probe verified the authenticity of the RT-PCR products (Figure 5A). Hence, out of the 15 cell lines tested, little or no expression of *RUNX3* could be detected in seven lines (47%). *RUNX3* expression in SNU16 cells was confirmed by Northern blotting, and the level of expression was found to be functionally saturated (see below). Therefore, SNU16 cells were considered to constitute a positive control for *RUNX3* expression.

In situ hybridization analysis showed that *RUNX3* expression was also greatly reduced in the clinical specimens (Figure 6). Figure 6D shows normal gastric mucosa, while Figure 6E shows cancer cells with irregularly shaped atypical tubular structures lined by pleomorphic cells and enlarged irregularly shaped vesicular nuclei. *RUNX3* expression can be clearly detected in normal gastric epithelial cells (Figure 6G) but only weakly in the cancer tissue (Figure 6H). Figure 6F shows a higher magnification of noncancerous mucosa marked F in Figure 6A. Interestingly, the left half of the tissue displays intestinal metaplasia, while the right half shows normal gastric mucosa. It is significant to note that *RUNX3* expression is greatly reduced in the metaplasia tissue compared with normal epithelial cells (Figure 6I). If intestinal metaplasia represents a precancerous state, the result would suggest that downregulation of *RUNX3* occurs at early stages of carcinogenic processes.

Of 22 stage I cases, 9 (41%) did not express *RUNX3* significantly. In the stage II, III, and IV cases, 1 out of 2 (50%), 11 out of 14 (79%), and 7 out of 8 (88%) exhibited reduction of *RUNX3* expression, respectively. With only one exception, all specimens having hemizygous deletions of *RUNX3* failed to express *RUNX3* at a detectable level ($p < 0.01$). In summary, *RUNX3* expression was reduced in 40% of early-stage carcinomas, and this level increased to nearly 90% with the advancement of the cancer stage ($p < 0.05$ examined by Mann-Whitney U test). On average, 60% of the clinical specimens showed reduced or no expression of *RUNX3* in the cancer tissue compared to the surrounding normal mucosa.

DNA Methylation of the Exon 1 Region of *RUNX3*
In cancer cells, the pattern of DNA methylation is often altered. Growing evidence suggests that aberrant DNA
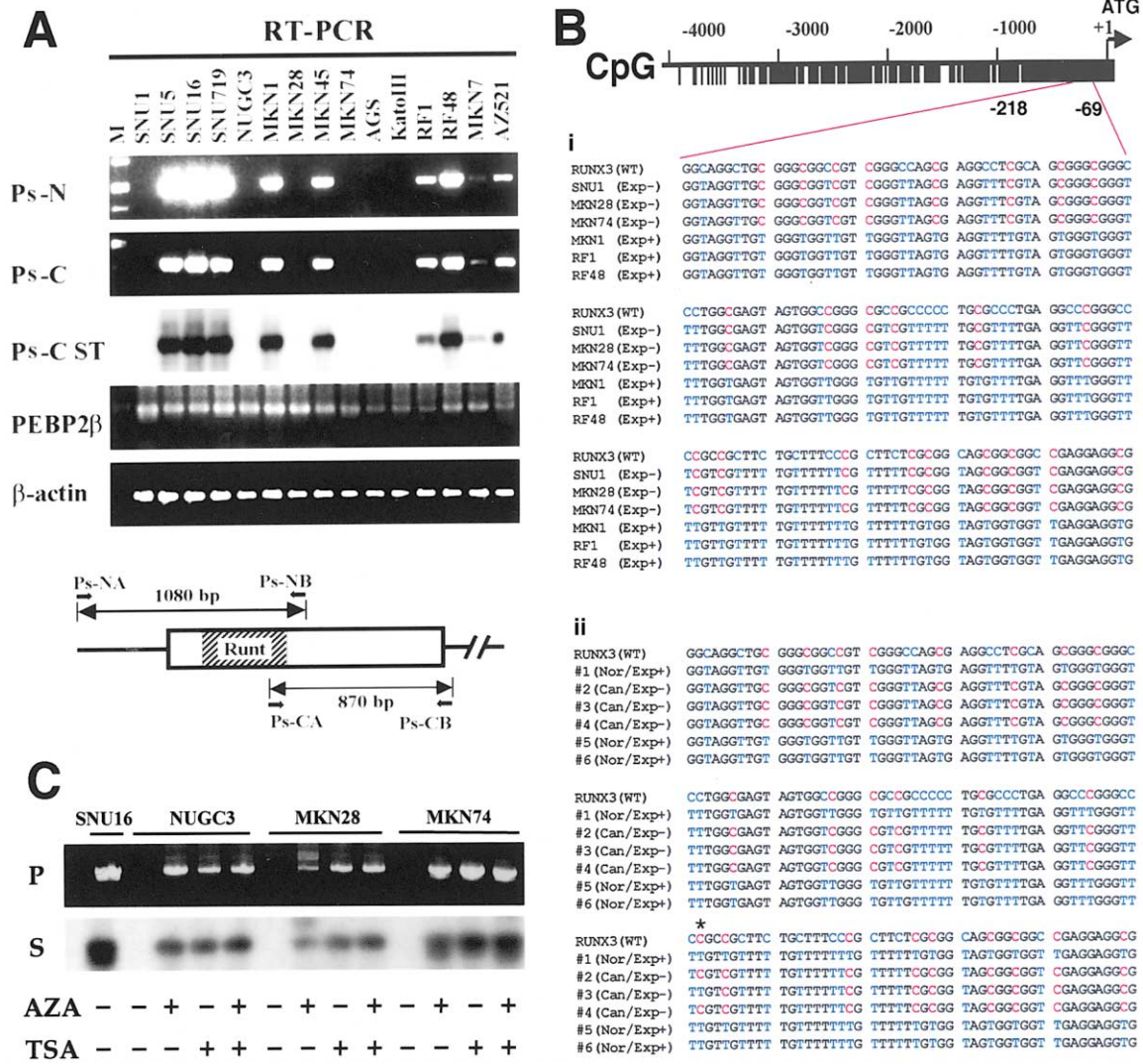
Figure 5. Frequent Reduction of *RUNX3* Expression in Gastric Cancer Cell Lines

(A) RT-PCR analysis of *RUNX3* expression patterns in gastric cancer cell lines. Gels: RT-PCR reaction with the primer pairs Ps-N and Ps-C, which cover the regions [Ps-NA and Ps-NB] and [Ps-CA and Ps-CB], respectively. The identity of the RT-PCR products obtained using the Ps-C primer pair was confirmed by Southern blotting (Ps-C ST) using the *RUNX3*-specific probe. The same first-strand cDNA preparations were subjected to RT-PCR amplification for PEBP2β and β-actin. Bottom: Schematic diagram of *RUNX3* cDNA in which the relative positions of the PCR primers are shown. The Runt domain is indicated by a hatched box (Runt).

(B) Methylation status of the C residues between −218 and −69 relative to the translation initiation site of the *RUNX3* exon 1 region. (i) The nucleotide sequences of the products of methylation-specific PCR of the DNA samples from the gastric cancer cell lines together with the wt *RUNX3* sequence at the top. The first three cell lines do not express RUNX3 (Exp−), while the remaining three express it (Exp+). The red C indicates that it was resistant to bisulfite treatment due to methylation. The blue T indicates that it was converted from C by bisulfite treatment, suggesting that the residue was not methylated. (ii) The nucleotide sequences of the products of methylation-specific PCR of the DNA samples from primary gastric cancer which do not express *RUNX3* (Can/Exp−) (#2, #3, and #4) and normal gastric mucosa which express *RUNX3* (Nor/Exp+) (#1, #5, and #6). Asterisk indicates that the C residue of #3 sample is not methylated at this position.

(C) Reactivation of *RUNX3* expression. Cells were cultured for 3 days in the presence of AZA (300 nM) or TSA (1 μM) or a mixture of both. Semiquantitative RT-PCR (see Experimental Procedures) was performed using the Ps-N primer set shown in (A), and the products were visualized by ethidium bromide staining (P) or Southern blotting (S) using *RUNX3* cDNA as a probe. Untreated SNU16 cells that express *RUNX3* were used as a control.

methylation of CpG islands around promoter regions can have the same effect as mutations in the coding regions on the inactivation of tumor-suppressor genes (Baylin et al., 2001). Since the promoter region of *RUNX3* contains a typical CpG island (GenBank accession number AL023096), we examined the methylation state of this region by digesting genomic DNA isolated from 15 cell lines with methylation-sensitive and -insensitive enzymes. The results showed a good correlation between a low-level or lack of expression of *RUNX3* and methylation in the vicinity of the *RUNX3* promoter (data not shown). We then directly examined the state of DNA methylation of six representative clones (three expressing and three not expressing *RUNX3*) by methylation-
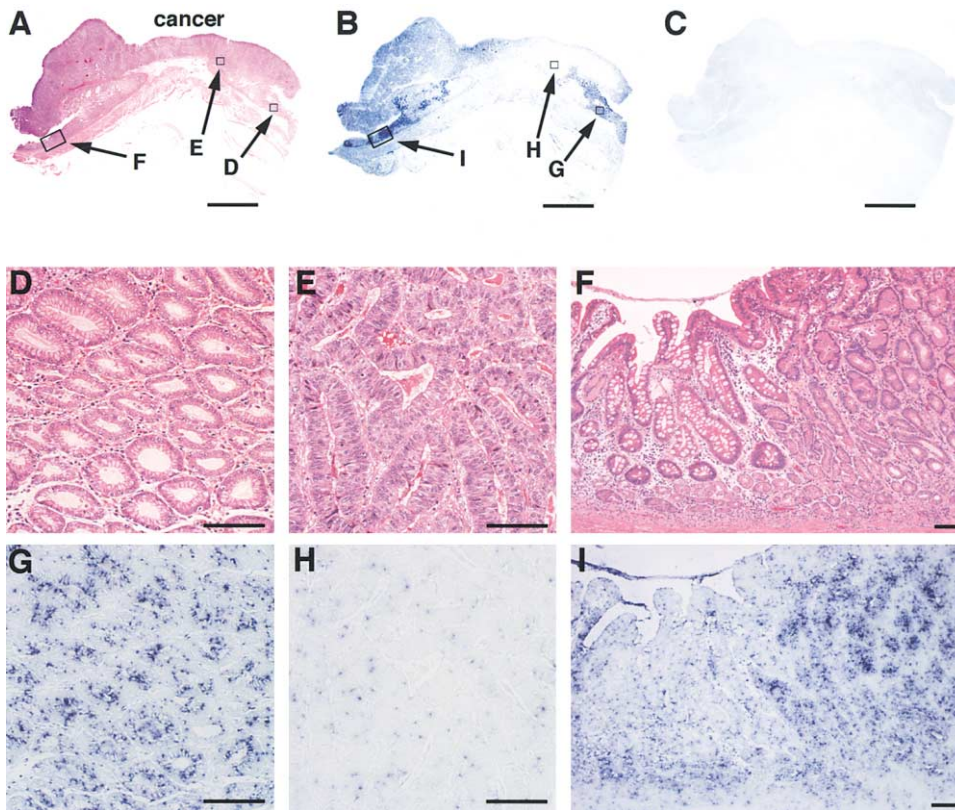
Figure 6. In Situ Hybridization of RUNX3 mRNA in a Primary Gastric Cancer Specimen

(A–C) HE staining (A) and in situ hybridization using an antisense probe (B) and a sense probe (C). Cancer tissue faces the lumen (upper side). Scale bars are equal to 5 mm.

(D–I) Enlargement of boxed regions marked (D)–(I) in (A) and (B). (D) and (G) show normal mucosa; (E) and (H) show cancer cells; (F) and (I) show a gastric tissue composed of normal mucosa (right half) and intestinal metaplasia (left half). Scale bars are 200 µm.

specific PCR. In three cell lines not expressing *RUNX3* (SNU1, MKN28, and MKN74), the C residues of the CpG dinucleotide sequence in the *RUNX3* exon 1 region were completely methylated, whereas those in three cell lines expressing *RUNX3* (MKN1, RF1, and RF48) were entirely methylation free (Figure 5B, i).

Three primary cancer specimens and three normal gastric mucosa specimens were also examined for the state of DNA methylation. Cancer specimens (#2, #3, #4) were all negative for *RUNX3* expression, and their C residues in the CpG dinucleotide within the region were methylated (Figure 5B, ii). In contrast, normal tissue samples (#1, #5, #6) were all positive for *RUNX3* expression (data not shown), and none of their C residues were methylated. The specimens #1 and #2 were obtained from the same patient. Therefore, the result reemphasizes our conclusion that gastric cancer cells do not express *RUNX3* due to hypermethylation of the exon 1 region, but normal epithelial cells surrounding the cancer tissue express *RUNX3* with methylation-free exon 1 region.

The silencing of gene expression by hypermethylation is due to recruitment of histone deacetylase to the methylated DNA (reviewed by Baylin et al., 2001). 5′-aza-2′-deoxycytidine (AZA), an inhibitor of DNA methyltransferase, and trichostatin A (TSA), an inhibitor of histone deacetylase, reactivate gene expression when hyper-

methylation of CpG islands is the cause of reduced gene expression (Cameron et al., 1999). To confirm that down-regulation of *RUNX3* expression is due to DNA methylation, the NUGC3, MKN28, and MKN74 cell lines were cultivated in the presence of AZA, TSA, or a combination of both. As shown in Figure 5C, expression of *RUNX3* was reactivated in all three cases to a level that was comparable to that of the control cell line, SNU16, consistent with the notion that hypermethylation of the CpG island of the *RUNX3* exon 1 region (Figure 5B) results in the inactivation of *RUNX3* expression.

Mutation in *RUNX3*

As in the case of hemizygous deletion, silencing by DNA methylation may have affected gene(s) other than *RUNX3*. To establish *RUNX3* as causally related to gastric carcinogenesis, we examined whether primary gastric cancers or cell lines derived from them bear mutations within the *RUNX3* coding region. By single-strand conformation polymorphism (SSCP) analysis, we screened 119 tumor tissues, including the 46 mentioned above.

Although mutations in *RUNX3* turned out to be rare, we found the C to T transition at C373 by which arginine 122 was converted to cysteine (R122C) was within the evolutionarily conserved Runt domain. Unfortunately, matching normal tissue was not available in this case and therefore, it was not possible to tell whether the
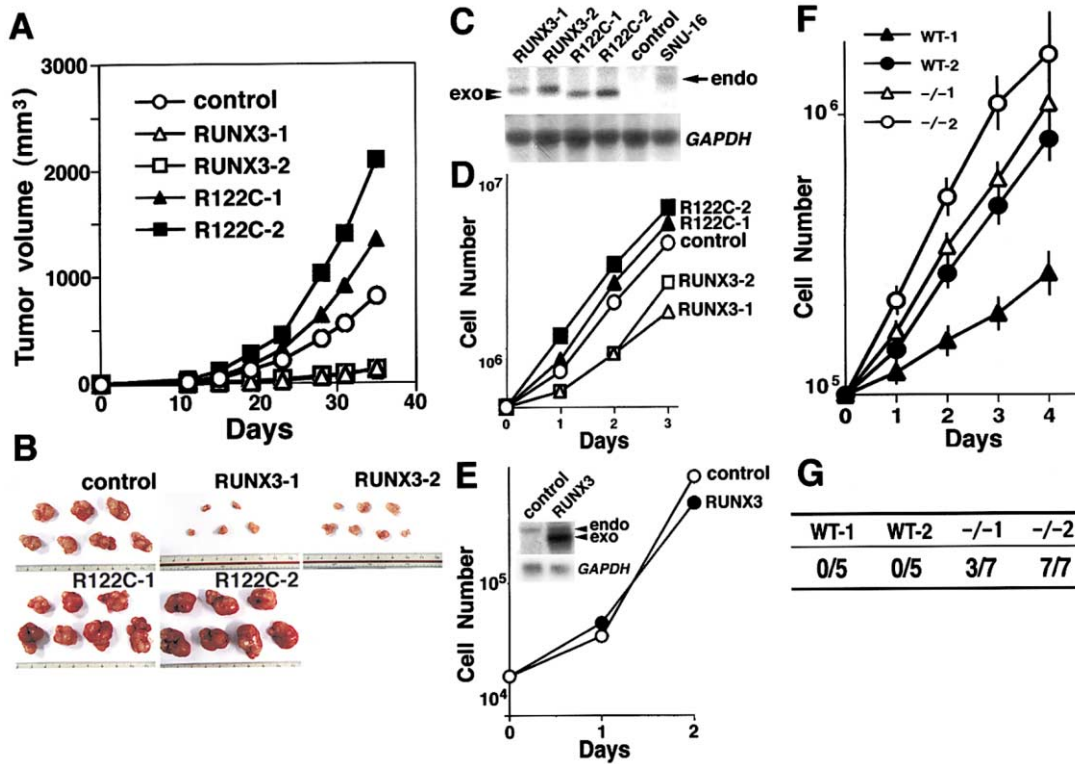
Figure 7. Inhibition of Tumorigenesis and In Vitro Cell Growth by *RUNX3*

(A) Tumorigenicity of MKN28 cells containing vector only (control), those expressing *RUNX3* clone 1 (RUNX3-1) or clone 2 (RUNX3-2), and those expressing *RUNX3 (R122C)* clone 1 (R122C-1) or clone 2 (R122C-2) were examined in nude mice. Cells were suspended in 0.85% phosphate-buffered saline (5×10^7 cells/ml), and 0.3 ml of cell suspension was injected subcutaneously.

(B) Tumors obtained at the end of the experiment shown in (A). Two mice injected with RUNX3-1 did not bear detectable tumors.

(C) Northern blot analysis of RNA extracted from cells described in (A) and SNU16. *RUNX3* cDNA was used as a probe.

(D) Growth curves of the cells in the monolayer culture.

(E) Growth curves of SNU16 cells (control) or SNU16 cells exogenously expressing *RUNX3* (RUNX3). Inset shows the levels of expression of endogenous (endo) and exogenous (exo) *RUNX3*.

(F) Growth curves of the cell lines in the monolayer culture.

(G) Tumor formation of WT-1, WT-2, −/−1, and −/−2 in nude mice 60 days after inoculation. Cells (1×10^7) of each cell line were inoculated into five (wt) or seven (−/−) mice. The number of mice bearing tumors is indicated above the number of mice used for the experiment.

change we observed was a single-nucleotide polymorphism or a true mutation. Nevertheless, it is important to note that arginine at position 122 is conserved in both nematodes and humans. Furthermore, the equivalent residue in RUNX2 has been shown to be mutated to glutamine in cleidocranial dysplasia (Zhou et al., 1999), suggesting that the mutation impairs an important function of RUNX proteins. We examined whether the mutation affects the tumor-suppressive activity of *RUNX3*.

Tumorigenesis Assay

The possible activity of *RUNX3* as a tumor suppressor was examined by a tumorigenesis assay in nude mice. MKN28 cells do not express *RUNX3* (Figure 5A) and formed rapidly growing tumors. Tumor growth was greatly reduced when exogenous *RUNX3* was stably expressed in the cells, suggesting that *RUNX3* has antioncogenic activity. On the other hand, the R122C mutation abolished the tumor-suppressor activity of *RUNX3*. Two independent *RUNX3(R122C)*-expressing MKN28 cell lines grew faster than the parental cells (Figures 7A and 7C). The tumors induced by MKN28 cells and their

derivatives obtained at the end of the experiment are shown in Figure 7B. It was interesting to note that, not only in vivo but also in vitro, *RUNX3*-expressing MKN28 cells grew more slowly than the parental cells, while *RUNX3(R122C)*-expressing MKN28 cells grew faster than *RUNX3*-expressing cells (Figure 7D). The expression level of exogenously introduced *RUNX3* was higher than that of endogenous *RUNX3* (Figure 7C). However, it is unlikely that the tumor-suppressive effect displayed by exogenous *RUNX3* is due to a nonspecific toxic effect induced by overexpression, since RUNX3(R122C), which differs from RUNX3 by only one amino acid out of 415 and displays a similar level expression, did not show any toxic effects. Furthermore, overexpression of *RUNX3* in the gastric cancer cell line SNU16, which does not have a deletion in the *RUNX3* locus and normally expresses *RUNX3*, did not affect significantly the growth of the cells (Figure 7E). The result suggests that *RUNX3* is a negative cell growth regulator both in vivo and in vitro and is consistent with the observation made with *RUNX3* null gastric epithelial cells.

If *RUNX3* is a tumor suppressor involved in gastric

carcinogenesis, *Runx3*$^{-/-}$ mice would be expected to acquire gastric cancer. As we mentioned earlier, however, *Runx3*$^{-/-}$ mice die soon after birth and therefore, we are unable to see any tumor growth. To overcome this problem, we obtained cell lines from epithelial cells of the glandular stomach of *Runx3*$^{-/-}$*p53*$^{-/-}$ as well as *Runx3*$^{+/+}$*p53*$^{-/-}$ mice. The reason for using the *p53* null mice was to enhance the chance of generating cell lines. As shown in Figure 7F, cell lines obtained from *Runx3*$^{-/-}$ mice grew faster on monolayer cultures than those from wt mice. More importantly, *Runx3*$^{-/-}$ cells induced tumors (adenocarcinoma) in nude mice, whereas *Runx3*$^{+/+}$ cells did not (Figure 7G).

Taken together, these results strongly suggest that *RUNX3* is a tumor-suppressor gene causally involved in gastric carcinogenesis.

Discussion

We demonstrated that *Runx3*, the third *runt*-related gene, is expressed in the glandular stomach epithelial cells, and *Runx3* null gastric mucosa develops hyperplasias due to promotion of proliferation and suppression of apoptosis in epithelial cells. Stimulated by these observations, we found silencing of *RUNX3* in about 60% of gastric cancer specimens examined. The level increased from 40% at early stages of cancer to almost 90% as the cancer stage progressed. About one-third of the cases at the earlier stages showed hemizygous deletion of *RUNX3*, the incidence of which also increased as the cancer stage advanced. Although rare, we found one mutation, *RUNX3(R122C)*, within the evolutionarily conserved Runt domain, pinpointing the importance of *RUNX3* as the gene inactivated by hemizygous deletions and by silencing due to DNA methylation. Furthermore, *RUNX3* displayed a tumor-suppressor effect in a tumorigenesis assay, and the *RUNX3(R122C)* mutation completely inactivated this effect. Finally, cell lines isolated from *Runx3*$^{-/-}$*p53*$^{-/-}$ mouse glandular stomach epithelium were tumorigenic in nude mice, whereas equivalent cell lines from *Runx3*$^{+/+}$*p53*$^{-/-}$ were not. These results strongly suggest that *RUNX3* is a tumor suppressor whose inactivation is involved in gastric carcinogenesis. It is also important to note that the phenotype of *Runx3*$^{-/-}$ mice was a subset of that described for *TGF-β1*$^{-/-}$ mice, suggesting that *Runx3* is an in vivo target of TGF-β signaling pathway demonstrated by animal experiments.

The human *RUNX3* gene is located on the short arm of human chromosome 1 at 1p36. The minimal deleted region in chromosome 1 from the gastric cancer cells is mapped between the genomic markers D1S119 and D1S246 (Ezaki et al., 1996). This region covers about 45 megabase pairs and contains about 200 genes, including *RUNX3*, but no known tumor suppressors.

Recently, it has been recognized that hypermethylation of the CpG island of the promoter region silences some genes as effectively as inactivation of the gene by mutations or deletions. These genes include *RB*, the von Hippel-Lindau gene, CDKN2A (*p16*^{INK4A}), CDKN2B (*p15*^{INK4B}), E cadherin (*E-cad*), *hMLH1*, *APC* (reviewed by Jones and Laird, 1999), and the caspase 8 gene (Teitz et al., 2000). *RUNX3* appears to be a new addition to the list.

In order to understand the antioncogenic activity of *RUNX3* in gastric cancer, it is worth considering the role of *RUNX1* in leukemogenesis. Sporadic and hereditary loss-of-function heterozygous mutations of *RUNX1* have been described (Osato et al., 1999; Song et al., 1999). Individuals who inherit heterozygous *RUNX1* mutation develop acute myeloid leukemia (AML) at very high frequency. Furthermore, biallelic loss of *RUNX1* is associated with a subtype of AML classified as FAB M0, suggesting that a complete loss of *RUNX1* causes a least-differentiated subtype of AML (Osato et al., 1999). A much larger percentage of AML cases are associated with the generation of leukemogenic chimeric proteins involving RUNX1 and PEBP2β/CBFβ. In these cases, ample evidence shows that the chimeric proteins almost always effectively inhibit the function of *RUNX1* (Cleary, 1999), strongly suggesting that the loss of *RUNX1* function is related to leukemogenicity. It is believed that *RUNX1* is essential for granulocytic differentiation and that loss of *RUNX1* function deprives myeloid progenitor cells of the capacity to differentiate but without harming their capacity for proliferation (Ito, 1999). This status of myeloid progenitor cells is considered to be the basis for the development of full-blown leukemia, which develops after the accumulation of other multiple genetic alterations. These observations suggest that *RUNX1* is a tumor suppressor for AML. As in the case of *RUNX1*, loss of *RUNX3* function may block differentiation pathways in stomach epithelium.

It is intriguing to note that *RUNX3* was found to be a negative growth regulator of gastric epithelial cells both from the *Runx3* knockout studies and from studies on gastric cancer. It is already known that *RUNX1* and *RUNX2* are involved in cell fate determination, that is, they are regulators of cell differentiation. It is of great interest to study the molecular mechanisms of regulation of cell growth and differentiation mediated by *RUNX3*.

The runt domain gene of *Caenorhabditis elegans*, known as *run*, is expressed in seam cells and intestinal cells. The seam cells, also known as lateral hypodermal cells, correspond to blast cells, which provide hypodermal nuclei and postdeirid neuroblasts; double-strand RNA interference that targeted the gene resulted in malformations of the hypodermis and intestine (Nam et al., 2002). This suggests that not only are Runt domain genes involved in the development of the functional gut, they also appear to be an evolutionarily conserved and important growth regulator of the gut. The gut is one of the most primitive organs in animals. That *Runx3*, of the three *Runx* genes present in mammals, appears to be the mediator of this task fits the picture in evolutionary terms, as comparison of the genomic structure of the *Runx* family genes suggests that *Runx3* is the most primitive of the three, and that the other two genes may have diverged from it. That is, *Runx3* is far smaller (about 70 kb) than the other *Runx* genes (more than 500 kb), and it lacks an exon present in *Runx1* and *Runx2* that is important for interacting with proteins such as Ets-1 (Bae et al., 1995).

RUNX3 was found to be silenced frequently in gastric cancer by hypermethylation of CpG islands in the exon 1 region. Reactivation of the genes silenced by DNA methylation by histone deacetylase inhibitors has been

described (Cameron et al., 1999). We have shown here that *RUNX3* was indeed reactivated by the combination of AZA and TSA. In this study, we have also shown that, although on average 30% of the cases of gastric cancer show hemizygous deletion of *RUNX3*, mutations and small deletions are very rare in the remaining allele or in either allele when both are silenced by hypermethylation. Therefore, in most cases, reactivation of *RUNX3* means reactivation of the gene without any mutations. Furthermore, exogenous expression of *RUNX3* in a cell line with a silenced *RUNX3* gene dramatically inhibited the tumor growth in nude mice. Together, these observations offer high hope that tumor growth in gastric cancer may potentially be controlled by inducing the expression of silenced *RUNX3* using reagents such as histone deacetylase inhibitors.

Experimental Procedures

Targeted Disruption of the *Runx3* Locus in Mice
A phage DNA clone containing exon 3 of the *Runx3* gene was isolated from a 129/SvJ mouse genomic library (Stratagene). The phage clone was used to generate a gene-targeting vector by introducing the *LacZ* gene into the *Sma*I site (12th codon in-frame) of exon 3. E14 mouse ES cells were cultured and transfected by electroporation with the plasmid as described previously (Gomi et al., 1995). Correctly targeted ES cells were injected into C57BL/6 blastocysts, and the resulting chimeras were crossed with C57BL/6 females.

β-Gal Staining and Histological Analyses
For whole-mount histochemical detection of β-gal activity, 12.5 dpc fetuses and 14.5 dpc gastrointestinal tracts were fixed with 4% paraformaldehyde and stained with X-gal cocktail as described (Huang et al., 1998). For histological analysis, tissues were fixed with 4% paraformaldehyde, embedded in paraffin, and sectioned at 6 μm. For immunohistochemical detection of active caspase 3, rabbit antibodies against active caspase 3 (R&D systems, AF835, 1 μg/ml) were used and visualized by incubation with biotin-conjugated second antibodies and then with streptavidin-FITC.

In Situ Hybridization
To detect *Runx3* expression in the mouse stomach, in situ hybridization was performed on 12 μm frozen sections as described previously (Satake et al., 1995) using sense and antisense digoxigenin (DIG)-labeled probes consisting of *Runx3* nucleotides (AF155880) −219 to 772 and 1023 to 1851. To detect *RUNX3* expression in human gastric cancer specimens, in situ hybridization on paraffin-embedded sections was performed as described previously (Yamada et al., 1997) using sense and antisense DIG-labeled probes consisting of *RUNX3* nucleotides 550–848.

Detection of Proliferating Cells
Proliferating cells were labeled with BrdU by using a BrdU Labeling and Detection Kit (Roche, 1299964). BrdU (30 mg/kg body weight) was injected i.v. into 18.5 dpc pregnant mice, and 4 hr later the fetal stomachs were fixed with 4% paraformaldehyde, embedded in paraffin, and sectioned at 6 μm.

Cell Lines and Cell Culture
Glandular stomach epithelia could be separated from mesenchymes using 30 mM EDTA-Hanks' solution (a modified method of Matsubara et al., 1998). Glandular stomach epithelial cells from each fetus were separately cultured in wells precoated with rat tail collagen gels in Ham's F12 medium with growth factors as previously reported (Fukamachi et al., 1994). TGF-β1 (3 ng/ml) was added to the culture medium at the start of the culture. Cell proliferation was determined on days 1 to 6 by a modification of the tetrazolium assay using MTT as a substrate as previously reported (Fukamachi, 1992). The relationship between genotype and epithelial responsiveness to TGF-β1 was determined by comparing the cell numbers in TGF-β1-supplemented and control cultures on day 3 when TGF-β1-induced

growth inhibition was highest. The results were analyzed statistically by the Mann-Whitney test and significance was set at $p < 0.05$. For the study of TGF-β1-induced apoptosis of glandular stomach epithelial cells, cells were cultured on Lab-Tek Chamber Glass Slides (Nalge Nunc, 177380) precoated with dried collagen substrata. Glandular stomach epithelial cells from each fetus were inoculated into wells and cultured as above. TGF-β1 (3 ng/ml) was added on day 4, and after 12 hr, cells were fixed with 4% paraformaldehyde for TUNEL analysis.

Gastric cancer cell lines (SNU1, SNU5, SNU16, SNU719, NUGC3, MKN1, MKN7, MKN28, MKN45, MKN74, KATOIII, and AZ521) were maintained in RPMI-1640 medium supplemented with 10% fetal bovine serum. RF1 and RF48 cells, and AGS cells were cultured in Leibovitz's L-15 and in F-12 medium supplemented with 10% fetal bovine serum, respectively.

$Runx3^{+/-}p53^{+/-}$ mice were mated to obtain $Runx3^{-/-}p53^{-/-}$ fetuses. Gastric epithelial cells were obtained from 16.5 dpc fetuses and cultured as above on collagen gels. Rapidly growing cells were subcultured on plastic and the cell lines, WT-1 and WT-2, were established from $Runx3^{+/+}p53^{-/-}$ mice while −/−1 and −/−2 were obtained from $Runx3^{-/-}p53^{-/-}$ mice.

Detection of Apoptotic Cells
Apoptotic cells were detected by the TUNEL method with a MEB-STAIN Apoptosis Kit Direct (MBL, 8445, Japan). Some cells were double-stained by TUNEL and propidium iodide to locate the nuclei.

Gastric Cancer Specimens
Primary gastric cancer tissues (119) were surgically resected. Of them, 71 were obtained from the Department of Digestive Surgery, Kyoto Prefectural University of Medicine, and 48 were obtained from the National Cancer Center Hospital, Tokyo. Of the total 119 clinical specimens, 46 had undegraded RNA and therefore, were used for in situ hybridization to examine the *RUNX3* RNA expression level and the integrity of the *RUNX3* genomic DNA. The remainder was a good source of DNA, although RNA was partially degraded, and was used for screening for mutations.

Plasmids and Stable Transfection
RUNX3(R122C) was created by site-directed mutagenesis from the human *RUNX3* cDNA (Bae et al., 1995). The wild-type and mutant *RUNX3* cDNAs (1775 bp and 1552 bp, respectively) were cloned into pcDNA3.1/HisC (Invitrogen) to generate the expression constructs, pcDNA3.1-*RUNX3* and pcDNA3.1-*RUNX3(R122C)*, respectively. Stable transfections were done with the Lipofectamine (GIBCO-BRL).

FISH
To detect copy number changes in *RUNX3*, FISH was carried out as described previously by Ishino et al. (1998). Two probes were used: pUCI.77 (specific for the pericentromeric regions of chromosome 1) and a *RUNX3* BAC clone (RP11-84-D-1), which contains 169 kb DNA including all of the exons of *RUNX3*. The PUC1.77 and RUNX3 BAC probes were labeled with bio-16-dUTP and dig-11-dUTP, respectively, by using a nick translation kit (Boehringer Mannheim). In normal peripheral blood cells, two spots of the centromere signal were detected in 93.1% ± 3.1%, and two spots of the *RUNX3* signal were detected in 96.2% ± 2.5%. We defined a hemizygous deletion of *RUNX3* as more than 20% of nuclei showing a *RUNX3*-to-centromere signal ratio of less than 1, as described by Ishino et al. (1998).

RT-PCR
cDNAs were synthesized from total RNA obtained from various gastric cancer cells using an oligo-dT primer according to the manufacturer's manual (GIBCO-BRL, Superscript kit). Using the cDNA as a template, *RUNX3* cDNA was amplified by the polymerase chain reaction (PCR) with two pairs of PCR primers, Ps-N (Ps-NA, 5'-CGC CACTTGATTCTGGAGGATTTGT-3'; Ps-NB, 5'-TGAAGTGGCTTGTG GTGCTGAGTGA-3') and Ps-C (Ps-CA, 5'-GAGTTTCACCCTGACCA TCACTGTG-3'; Ps-CB, 5'-GCCCATCACTGGTCTTGAAGGTTGT-3'). To confirm the integrity of the prepared RNA, the same cDNAs were subjected to PCR amplification of *PEBP2β/CBFB* and β-*actin* cDNA.

When rough quantification was required, semiquantitative PCR was performed by removing two reaction cycles from the minimum saturating reaction cycle.

SSCP

To detect *RUNX3* mutations in clinical samples, SSCP analysis was performed using the following primers: Exon1-F, 5′-GGGAAGCCGCGC CGTCTCC-3′; Exon1-R, 5′-CGAGGCTCTGGCTCCCGCAGC-3′ (406 bp); Exon2-F, 5′-TAAGCTGTCCCCCTGCATCC-3′; Exon2-R: 5′-CAAT GCTGAAATGGCGAGGC-3′ (231 bp); Exon3-F, 5′-GCCAACCGCCTGC CTCTATT-3′; Exon3-R, 5′-AGGGGGCTCGGTGGCACTT-3′ (161 bp); Exon4-F, 5′-TCTGGGGAAGCAACGGCTGA-3′; Exon4-R, 5′-CAGCCC CTCCCTCCGTG-3′ (223 bp); Exon5-F,5′-GAGCCAGGTCTAGAACT AGG-3′; and Exon5-R, 5′-TTGAAGGTTGTTAGGGTCC-3′ (721 bp). The PCR products for exon 1 and exon 5 were digested with *Apa*I and *Sph*I, respectively. The PCR products or restricted PCR products were applied to gels with or without glycerol, as described previously (Ushijima et al., 1995).

Methylation-Specific PCR

Methylation-specific PCR was performed as reported previously (Herman et al., 1996). Briefly, genomic DNA denatured by NaOH was treated with sodium bisulfite and purified. The DNA was subjected to PCR using following primers. The primer set used for untreated DNA: Rx3-5W (5′-GAGGGGCGGCCGCACGCGGG-3′), Rx3-3W (5′-CGGCCGGC GCGGGCGCCTCC-3′). The primer set used for detecting methylated DNA: Rx3-5M (5′-TTACGAGGGGCGGTCGTACGCGGG-3′), Rx3-3M (5′-AAAACGACCGACGCGAACGCCTCC-3′). The primer set used for detecting unmethylated DNA: Rx3-5U (5′-TTATGAGGGGTGGTTGTAT GTGGG-3′), Rx3-3U (5′-AAAACAACCAACACAAACACCTCC-3′). Methylated nucleotides were verified by sequencing the PCR products.

References

Bae, S.-C., Takahashi, E., Zhang, Y.W., Ogawa, E., Shigesada, K., Namba, Y., Satake, M., and Ito, Y. (1995). Cloning, mapping and expression of PEBP2αC, a third gene encoding the mammalian Runt domain. Gene *159*, 245–248.

Baylin, S.B., Esteller, M., Rountree, M.R., Bachman, K.E., Schuebel, K., and Herman, J.G. (2001). Aberrant patterns of DNA methylation, chromatin formation and gene expression in cancer. Hum. Mol. Genet. *10*, 687–692.

Cameron, E.E., Bachman, K.E., Myohanen, S., Herman, J.G., and Baylin, S.B. (1999). Synergy of demethylation and histone deacetylase inhibition in the re-expression of genes silenced in cancer. Nat. Genet. *21*, 103–107.

Cleary, M.L. (1999). A new angle on a pervasive oncogene. Nat. Genet. *23*, 134–135.

Crawford, S.E., Stellmach, V., Murphy-Ullrich, J.E., Ribeiro, S.M., Lawler, J., Hynes, R.O., Boivin, G.P., and Bouck, N. (1998). Thrombospondin-1 is a major activator of TGFβ1 in vivo. Cell *93*, 1159–1170.

Ezaki, T., Yanagisawa, A., Ohta, K., Aiso, S., Watanabe, M., Hibi, T.,

Kato, Y., Nakajima, T., Ariyama, T., Inazawa, J., et al. (1996). Deletion mapping on chromosome 1p in well-differentiated gastric cancer. Br. J. Cancer *73*, 424–428.

Fukamachi, H. (1992). Proliferation and differentiation of fetal rat intestinal epithelial cells in primary serum-free culture. J. Cell Sci. *103*, 511–519.

Fukamachi, H., Ichinose, M., Ishihama, S., Tsukada, S., Yasugi, S., Shiokawa, K., Furihata, C., Yonezawa, S., and Miki, K. (1994). Fetal rat glandular stomach epithelial cells differentiate into surface mucous cells which express cathepsin E in the absence of mesenchymal cells in primary culture. Differentiation *56*, 83–89.

Fukushige, S., Matsubara, K., Yoshida, M., Sasaki, M., Suzuki, T., Semba, K., Toyoshima, K., and Yamamoto, T. (1986). Localization of a novel v-erbB-related gene, c-erbB-2, on human chromosome 17 and its amplification in a gastric cancer cell line. Mol. Cell. Biol. *6*, 955–958.

Gomi, H., Yokoyama, T., Fujimoto, K., Ikeda, T., Katoh, A., Itoh, T., and Itohara, S. (1995). Mice devoid of the glial fibrillary acidic protein develop normally and are susceptible to scrapie prions. Neuron *14*, 29–41.

Guilford, P., Hopkins, J., Harraway, J., McLeod, M., McLeod, N., Harawira, P., Taite, H., Scoular, R., Miller, A., and Reeve, A.E. (1998). E-cadherin germline mutations in familial gastric cancer. Nature *392*, 402–405.

Hanai, J., Chen, L.-F., Kanno, T., Ohtani-Fujita, N., Kim, W.-Y., Guo, W.-H., Imamura, T., Ishidou, Y., Fukuchi, M., Shi, M.-J., et al. (1999). Interaction and functional cooperation of PEBP2/CBF with Smads. Synergistic induction of the immunoglobulin germline Calpha promoter. J. Biol. Chem. *274*, 31577–31582.

Herman, J.G., Graff, J.R., Myohanen, S., Nelkin, B.D., and Baylin, S.B. (1996). Methylation-specific PCR: a novel PCR assay for methylation status of CpG islands. Proc. Natl. Acad. Sci. USA *93*, 9821–9826.

Huang, D., Chen, S.W., Langston, A.W., and Gudas, L.J. (1998). A conserved retinoic acid responsive element in the murine Hoxb-1 gene is required for expression in the developing gut. Development *125*, 3235–3246.

Ishino, S., Hashimoto, N., Fushiki, S., Date, K., Mori, T., Fujimoto, M., Nakagawa, Y., Ueda, S., Abe, T., and Inazawa, J. (1998). Loss of material from chromosome arm 1p during malignant progression of meningioma revealed by fluorescent in situ hybridization. Cancer *83*, 360–366.

Ito, Y. (1999). Molecular basis of tissue-specific gene expression mediated by the runt domain transcription factor PEBP2/CBF. Genes Cells *4*, 685–696.

Jones, P.A., and Laird, P.W. (1999). Cancer epigenetics comes of age. Nat. Genet. *21*, 163–167.

Kim, J.H., Takahashi, T., Chiba, I., Park, J.G., Birrer, M.J., Roh, J.K., De Lee, H., Kim, J.P., Minna, J.D., and Gazdar, A.F. (1991). Occurrence of p53 gene abnormalities in gastric carcinoma tumors and cell lines. J. Natl. Cancer Inst. *83*, 938–943.

Kuniyasu, H., Yasui, W., Yokozaki, H., Akagi, M., Akama, Y., Kitahara, K., Fujii, K., and Tahara, E. (1994). Frequent loss of heterozygosity of the long arm of chromosome 7 is closely associated with progression of human gastric carcinomas. Int. J. Cancer *59*, 597–600.

Lee, B., Thirunavukkarasu, K., Zhou, L., Pastore, L., Baldini, A., Hecht, J., Geoffroy, V., Ducy, P., and Karsenty, G. (1997). Missense mutations abolishing DNA binding of the osteoblast-specific transcription factor OSF2/CBFA1 in cleidocranial dysplasia. Nat. Genet. *16*, 307–310.

Look, A.T. (1997). Oncogenic transcription factors in the human acute leukemias. Science *278*, 1059–1064.

Matsubara, Y., Ichinose, M., Yahagi, N., Tsukada, S., Oka, M., Miki, K., Kimura, S., Omata, M., Shiokawa, K., Kitamura, N., et al. (1998). Hepatocyte growth factor activator: a possible regulator of morphogenesis during fetal development of the rat gastrointestinal tract. Biochem. Biophys. Res. Commun. *253*, 477–484.

Mundlos, S., Otto, F., Mundlos, C., Mulliken, J.B., Aylsworth, A.S., Albright, S., Lindhout, D., Cole, W.G., Henn, W., Knoll, J.H., et al.

(1997). Mutations involving the transcription factor CBFA1 cause cleidocranial dysplasia. Cell *89*, 773–779.

Nam, S.-H., Jin, Y.-H., Li, Q.-L., Ito, Y., Lee, J., and Bae, S.-C. (2002). Expression pattern, regulation, and biological role of runt domain transcription factor, *run*, in *Caenorhabditis elegans*. Mol. Cell. Biol. *22*, 547–554.

Okuda, T., van Dursen, J., Hiebert, S.W., Grosweld, G., and Downing, J.R. (1996). AML1, the target of multiple chromosomal translocation in human leukemia, is essential for normal fetal liver hematopoiesis. Cell *84*, 321–330.

Osato, M., Asou, N., Abdalla, E., Hoshino, K., Yamasaki, H., Okubo, T., Suzushima, H., Takatsuki, K., Kanno, T., Shigesada, K., and Ito, Y. (1999). Biallelic and heterozygous point mutations in the runt domain of the AML1/PEBP2alphaB gene associated with myeloblastic leukemias. Blood *93*, 1817–1824.

Park, K., Kim, S.-J., Bang, Y.-J., Park, J.-G., Kim, N.K., Roberts, A.B., and Sporn, M.B. (1994). Genetic changes in the transforming growth factor beta (TGF-beta) type II receptor gene in human gastric cancer cells: correlation with sensitivity to growth inhibition by TGF-beta. Proc. Natl. Acad. Sci. USA *91*, 8772–8776.

Parkin, D.M., Whelan, S.L., Ferlay, J., Raymond, L., and Young, J. (1997). Cancer Incidence in Five Continents, Volume VII (Lyon, France: IARC Scientific Publications No. 143).

Parkin, D.M., Pisani, P., and Ferlay, J. (1999). Estimates of the worldwide incidence of 25 major cancers in 1990. Int. J. Cancer *80*, 827–841.

Rege-Cambrin, G., Scaravaglio, P., Carozzi, F., Giordano, S., Ponzetto, C., Comoglio, P.M., and Saglio, G. (1992). Karyotypic analysis of gastric carcinoma cell lines carrying an amplified c-met oncogene. Cancer Genet. Cytogenet. *64*, 170–173.

Sano, T., Tsujino, T., Yoshida, K., Nakayama, H., Haruma, K., Ito, H., Nakamura, Y., Kajiyama, G., and Tahara, E. (1991). Frequent loss of heterozygosity on chromosomes 1q, 5q, and 17p in human gastric carcinomas. Cancer Res. *51*, 2926–2931.

Satake, M., Nomura, S., Yamaguchi-Iwai, Y., Takahama, Y., Hashimoto, Y., Niki, M., Kitamura, Y., and Ito, Y. (1995). Expression of the Runt domain-encoding PEBP2α genes in T cells during thymic development. Mol. Cell. Biol. *15*, 1662–1670.

Sobin, I.H., and Wittekind, C.H. (1997). TNM Classification of Malignant Tumors, 5th ed. (New York: International Union Against Cancer [UICC]).

Song, W.-J., Sullivan, M.G., Legare, R.D., Hutchings, S., Tan, X., Kufrin, D., Ratajczak, J., Resende, I.C., Haworth, C., Hock, R., et al. (1999). Haploinsufficiency of CBFA2 causes familial thrombocytopenia with propensity to develop acute myelogenous leukaemia. Nat. Genet. *23*, 166–175.

Tamura, G., Kihana, T., Nomura, K., Terada, M., Sugimura, T., and Hirohashi, S. (1991). Detection of frequent p53 gene mutations in primary gastric cancer by cell sorting and polymerase chain reaction single-strand conformation polymorphism analysis. Cancer Res. *51*, 3056–3058.

Teitz, T., Wei, T., Valentine, M.B., Vanin, E.F., Grenet, J., Valentine, V.A., Behm, F.G., Look, A.T., Lahti, J.M., and Kidd, V.J. (2000). Caspase 8 is deleted or silenced preferentially in childhood neuroblastomas with amplification of MYCN. Nat. Med. *6*, 529–535.

Uchino, S., Tsuda, H., Noguchi, M., Yokota, J., Terada, M., Saito, T., Kobayashi, M., Sugimura, T., and Hirohashi, S. (1992). Frequent loss of heterozygosity at the DCC locus in gastric cancer. Cancer Res. *52*, 3099–3102.

Ushijima, T., Hosoya, Y., Suzuki, T., Sofuni, T., Sugimura, T., and Nagao, M. (1995). A rapid method for detection of mutations in the *lacI* gene using PCR-single strand conformation polymorphism analysis: demonstration of its high sensitivity. Mutat. Res. *334*, 283–292.

Yamada, K., Matsuki, M., Morishima, Y., Ueda, E., Tabata, K., Yasuno, H., Suzuki, M., and Yamanishi, K. (1997). Activation of the human transglutaminase 1 promoter in transgenic mice: terminal differentiation-specific expression of the TGM1-lacZ transgene in keratinized stratified squamous epithelia. Hum. Mol. Genet. *6*, 2223–2231.

Zhou, G., Chen, Y., Zhou, L., Thirunavukkarasu, K., Hecht, J., Chitayat, D., Gelb, B.D., Pirinen, S., Berry, S.A., Greenberg, C.R., et al. (1999). CBFA1 mutation analysis and functional correlation with phenotypic variability in cleidocranial dysplasia. Hum. Mol. Genet. *8*, 2311–2316.